Thermoelectric transport within density functional theory

Nahual Sobrino,[1,2,*] Florian Eich,[3] Gianluca Stefanucci,[4,5] Roberto D'Agosta,[2,6,†] and Stefan Kurth[2,6,1,‡]

[1]*Donostia International Physics Center, Paseo Manuel de Lardizabal 4, E-20018 San Sebastián, Spain*
[2]*Nano-Bio Spectroscopy Group and European Theoretical Spectroscopy Facility (ETSF), Departamento de Polímeros y Materiales Avanzados: Física, Química y Tecnología, Universidad del País Vasco UPV/EHU, Avenida de Tolosa 72, E-20018 San Sebastián, Spain*
[3]*HQS Quantum Simulations GmbH, Haid-und-Neu-Straße 7, D-76131 Karlsruhe, Germany*
[4]*Dipartimento di Fisica, Università di Roma Tor Vergata, Via della Ricerca Scientifica 1, 00133 Rome, Italy;*
European Theoretical Spectroscopy Facility (ETSF)
[5]*INFN, Laboratori Nazionali di Frascati, Via E. Fermi 40, 00044 Frascati, Italy*
[6]*IKERBASQUE, Basque Foundation for Science, Plaza de Euskadi 5, E-48009 Bilbao, Spain*

A formalism to describe steady-state electronic and thermal transport in the framework of density functional theory is presented. A one-to-one correspondence is proven between the three basic variables of the theory, i.e., the density on as well as the electrical and heat currents through the junction, and the three basic potentials, i.e., the local potential in as well as the DC bias and thermal gradient across the junction. Consequently, the Kohn-Sham system of the theory requires three exchange-correlations potentials. In linear response, the formalism leads to exact expressions for the many-body transport coefficients (both electrical and thermal conductances and Seebeck coefficient) in terms of both the corresponding Kohn-Sham coefficients and derivatives of the exchange-correlations potentials. The theory is applied to the single impurity Anderson model and an accurate analytic parametrization for these derivatives in the Coulomb blockade regime is constructed through reverse engineering.

I. INTRODUCTION

Thermoelectricity [1] is at the heart of a range of technological applications, e.g., energy conversion, and is intrinsically related to both charge and heat transport. With progress in the manipulation and fabrication of materials at the nanoscale and even at the level of single molecules (molecular electronics, see Refs. [2–6]), designing more efficient thermoelectrics requires reliable modeling techniques at an atomistic level. Today, density functional theory (DFT) is most often the method of choice for *ab initio* modeling due to its favorable balance of accuracy and numerical efficiency. In a DFT framework, transport is typically described by combining DFT with the Landauer-Büttiker (LB) approach. This LB-DFT formalism, also known as DFT-NEGF (DFT plus nonequilibrium Green's function), treats transport as a scattering problem of noninteracting electrons. The resulting Landauer formula for the electronic current is physically very intuitive in that the current is given as an energy integral of the transmission function integrated over the bias window. The LB-DFT framework has become extremely useful in a qualitative understanding of transport through, e.g., single molecules.

However, one should keep in mind that the noninteracting nature of electrons in LB-DFT clearly is an approximation. Furthermore, LB-DFT uses ground-state (equilibrium) DFT in a nonequilibrium situation (transport) which is formally not justified.

A proper nonequilibrium DFT approach to transport could be time-dependent DFT (TDDFT) [7] where the steady state is achieved in the long-time limit of the time evolution of the system after switching on a DC bias. Formally, the long-time limit of TDDFT leads to exchange-correlation (xc) corrections to the bias [8–13] which are absent in LB-DFT but are difficult to model. Within TDDFT, one can hope to describe the (longitudinal) part of the electronic (steady) current. For the additional description of heat (or energy) currents, the formalism has been extended recently [14–16], but applications have so far been restricted to noninteracting systems [17] due to the lack of approximations to the corresponding xc functionals.

Recently, an alternative DFT approach to transport in the steady state was suggested [18]. This so-called i-DFT formalism allows us to compute the steady-state density and electronic current (and thus the electrical conductance). Again, just like in TDDFT, this is achieved via an xc contribution to the bias. Unlike in TDDFT, however, xc functionals have been constructed for nontrivial model systems such as the single impurity Anderson model (SIAM), both in the Kondo as well as in the Coulomb blockade regime [19]. Also, in TDDFT the exact xc functional has memory dependence [20–25] whereas the i-DFT xc functionals only depend on the steady-state values of the densities. Somewhat unexpectedly, i-DFT can also be used to compute many-body spectral functions both in [26,27] and out of equilibrium [28].

By construction, i-DFT does not give access to the heat current (although the Seebeck coefficient can be extracted [29]).

*nahualcsc@dipc.org
†roberto.dagosta@ehu.es
‡stefan.kurth@ehu.es

125115-1

In the present paper, we will close this gap and generalize i-DFT to iq-DFT, a formalism which allows us to compute not only the (steady-state) density and electrical current but also the electronic contribution to the heat current.

The structure of the paper is as follows: In Sec. II, we prove the fundamental theorem of the iq-DFT formalism (the one-to-one correspondence between densities and potentials) and introduce the corresponding Kohn-Sham (KS) scheme. In Sec. III, we derive the linear response equations which allow expressing the linear transport coefficients solely in terms of iq-DFT quantities. These coefficients include the thermal conductance, for which up to now only the (formally incomplete) LB-DFT expression has been available. In Sec. IV, we apply iq-DFT to the SIAM in the linear response regime. From reverse engineering, we derive analytic parametrizations for all iq-DFT quantities needed to describe the Anderson model in the Coulomb blockade regime. In the Appendix, we give detailed derivations for the analytical integrals needed in Sec. IV.

II. FORMALISM

We consider the typical setup for electronic transport which consists of a central molecular junction (C) coupled to a left (L) and a right (R) electrode. The electrodes are in (local) thermal equilibrium with temperatures $T_{L/R}$ and chemical potentials $\mu_{L/R}$, respectively. The central region C is subject to an electrostatic potential $v(\mathbf{r})$ generated by, e.g., the nuclei in the molecular junction and/or an external gate potential which vanishes deep inside the electrodes. The system can be driven out of equilibrium by a finite thermal gradient $\Delta T = T_L - T_R$ and/or an external DC bias V across the junction. We assume that these perturbations in the long-time limit lead to a steady-state electrical current (I) as well as energy and heat currents (W and Q, respectively).

We aim to construct a formally exact density functional framework, which we call iq-DFT, to describe such a steady state and reproduce these currents. To this end, we extend the recently proposed DFT framework for steady-state transport [18], also called i-DFT, which in principle captures the steady-state density $n(\mathbf{r})$ in the central region C, as well as the steady current I through it. By construction, in the linear-response regime, i-DFT gives access to the (many-body) electrical conductance and can also describe the Seebeck coefficient [29]. On the other hand, the energy or heat currents are not guaranteed to be reproduced in i-DFT and therefore also the thermal conductance is not captured. i-DFT is based on the one-to-one map between the pair of densities $(n(\mathbf{r}), I)$ and the pair of potentials $(v(\mathbf{r}), V)$, where the bias V across region C is given as $V = \mu_L - \mu_R$.

In our iq-DFT framework for the description of both charge *and* thermal transport, we establish a one-to-one map between the three densities $(n(\mathbf{r}), I, Q)$ and the three potentials $(v(\mathbf{r}), V, \Psi)$, where $\Psi = (T_L - T_R)/T$ is the normalized thermal gradient and $T = (T_L + T_R)/2$ is the background temperature. In linear response, iq-DFT gives access not only to the electrical conductance and the Seebeck coefficient but also to the thermal conductance, see Sec. III.

In the following, we adopt the sign convention that currents flowing into the central region are positive. Due to charge

and energy conservation, the steady-state electrical/energy current flowing in from the left lead is equal to the steady-state electrical/energy current flowing out through the right lead, i.e., $I \equiv I_L = -I_R$ (electrical current), $W \equiv W_L = -W_R$ (energy current) and $Q \equiv Q_L = -IV - Q_R$ (heat current).

The foundation of iq-DFT rests on the following theorem which establishes the one-to-one correspondence between the basic variables of the theory $(n(\mathbf{r}), I, Q)$ and the three driving forces or potentials $(v(\mathbf{r}), V, \Psi)$.

Theorem: For any finite temperature T and fixed electrostatic potential in the leads, there exists a one-to-one correspondence between the set of densities $(n(\mathbf{r}), I, Q)$ and the set of potentials $(v(\mathbf{r}), V, \Psi)$ in a (gate dependent) finite region of bias and thermal gradient around $V = 0$ and $\Psi = 0$.

Proof: The existence of the invertible map can be proven by showing that the determinant of the Jacobian

$$J = \det \begin{pmatrix} \frac{\delta n(\mathbf{r})}{\delta v(\mathbf{r}')} & \frac{\partial n(\mathbf{r})}{\partial V} & \frac{\partial n(\mathbf{r})}{\partial \Psi} \\ \frac{\delta I}{\delta v(\mathbf{r}')} & \frac{\partial I}{\partial V} & \frac{\partial I}{\partial \Psi} \\ \frac{\delta Q}{\delta v(\mathbf{r}')} & \frac{\partial Q}{\partial V} & \frac{\partial Q}{\partial \Psi} \end{pmatrix} \Bigg|_{\substack{V=0 \\ \Psi=0}} \tag{1}$$

is nonvanishing.

Since a change in the gate voltage cannot produce a persistent current in the linear regime, we have

$$\frac{\delta I}{\delta v(\mathbf{r})}\Bigg|_{\substack{V=0 \\ \Psi=0}} = 0, \qquad \frac{\delta Q}{\delta v(\mathbf{r})}\Bigg|_{\substack{V=0 \\ \Psi=0}} = 0, \tag{2}$$

and therefore we can write Eq. (1) as

$$J = \det(\chi(\mathbf{r}, \mathbf{r}'))\det(\mathbf{L}) = \det(\chi(\mathbf{r}, \mathbf{r}'))TG\kappa, \tag{3}$$

where $\chi(\mathbf{r}, \mathbf{r}') = \frac{\delta n(\mathbf{r})}{\delta v(\mathbf{r}')}\big|_{\substack{V=0 \\ \Psi=0}}$ is the static equilibrium density response function and G and κ are the electrical and thermal conductances. These are derived from the linear response relationship between the currents (I, Q) which, to first order, result from application of the potentials (V, Ψ),

$$\begin{pmatrix} I \\ Q \end{pmatrix} = \mathbf{L}\begin{pmatrix} V \\ \Psi \end{pmatrix} = \begin{pmatrix} L_{11} & L_{12} \\ L_{21} & L_{22} \end{pmatrix}\begin{pmatrix} V \\ \Psi \end{pmatrix}, \tag{4}$$

with $L_{21} = L_{12}$ from Onsager's relation [30]. The conductance matrix $\mathbf{L}$ can be expressed in terms of the transport coefficients as [31]

$$\mathbf{L} = \begin{pmatrix} G & -TGS \\ -TGS & T\kappa + T^2GS^2 \end{pmatrix}, \tag{5}$$

where S is the Seebeck coefficent. Equivalently, we can use Eq. (5) to express the transport coefficients in terms of the matrix elements L_{ij} as

$$G = \frac{\partial I}{\partial V}\Bigg|_{\substack{V=0 \\ \Psi=0}} = L_{11}, \tag{6a}$$

$$S = \frac{\partial V}{\partial \Delta T}\Bigg|_{\substack{I=0 \\ Q=0}} = -\frac{1}{T}\frac{L_{12}}{L_{11}}, \tag{6b}$$

$$\kappa = -\frac{\partial Q}{\partial \Delta T}\Bigg|_{\substack{I=0 \\ Q=0}} = \frac{1}{T}\left(L_{22} - \frac{L_{12}^2}{L_{11}}\right). \tag{6c}$$

It has already been shown [18] that, for any finite temperature T, we have $\det(\chi(\mathbf{r}, \mathbf{r}')) < 0$ [18] and $G > 0$ [18,32]. There-

fore, to complete the proof of the theorem, it remains to be shown that $\kappa > 0$.

This step can be done by applying Onsager's original arguments. In the steady state, the time-derivative of the entropy $\mathcal{S}$ in the central molecular region equals the sum of the entropy currents Q_α/T, $\alpha = L, R$, from the leads

$$\dot{\mathcal{S}} = -\left(\frac{Q_L}{T_L} + \frac{Q_R}{T_R}\right)$$
$$= -\frac{1}{T}\left(Q_L + Q_R - \frac{\Psi}{2}(Q_L - Q_R)\right), \quad (7)$$

where the minus sign follows from our convention that currents flowing into the central region C are positive. In the last step, we expanded to linear order for small temperature gradients Ψ. Using the relation

$$W_\alpha = Q_\alpha + \mu_\alpha I_\alpha \quad (8)$$

between energy and heat currents, and using that in the steady state we have $I_L = -I_R = I$ and $W_L = -W_R = W$, we arrive at

$$\dot{\mathcal{S}} = \frac{1}{T}(IV + Q\Psi)$$
$$= \frac{1}{T}(L_{11}V^2 + 2L_{12}V\Psi + L_{22}\Psi^2), \quad (9)$$

where we used Eq. (4) in the last step.

From the second law of the thermodynamics, we know that $\dot{\mathcal{S}} \geqslant 0$, where the equality sign holds at equilibrium. Therefore, the equilibrium state of the system corresponds to the local minimum of the rate of production of entropy. As a consequence, the determinant of the Hessian matrix of $\dot{\mathcal{S}}$ has to be positive around $V = 0$, $\Psi = 0$:

$$\mathbf{H}_{\dot{\mathcal{S}}} = \left.\frac{\partial^2\dot{\mathcal{S}}}{\partial V^2}\right|_{\substack{V=0\\\Psi=0}} \left.\frac{\partial^2\dot{\mathcal{S}}}{\partial\Psi^2}\right|_{\substack{V=0\\\Psi=0}} - \left.\frac{\partial^2\dot{\mathcal{S}}}{\partial V\partial\Psi}\right|_{\substack{V=0\\\Psi=0}}^2$$
$$= \frac{4}{T^2}\left(L_{11}L_{22} - L_{12}^2\right) = 4T^{-1}G\kappa > 0. \quad (10)$$

From Eq. (10), the positiveness of the thermal conductance $\kappa > 0$ directly follows, which completes the proof of the one-to-one map.

An equivalent formulation stems from considering as a third basic variable the energy current W instead of Q. The theory thus leads to a one-to-one correspondence between $(n(\mathbf{r}), I, W)$ and the trio of potentials $(v(\mathbf{r}), V - \mu_L\Psi, \Psi)$. The two formulations are related through Eq. (8) [33].

A. Kohn-Sham equations of iq-DFT

The iq-DFT theorem holds for any form of the interaction, in particular, also for the noninteracting case. To establish the KS scheme, we make the usual assumption of noninteracting representability, i.e., that there exists a unique trio of potentials $(v_s(\mathbf{r}), V_s, \Psi_s)$ for a noninteracting system, the KS system, which exactly reproduces the densities $(n(\mathbf{r}), I, Q)$ of the interacting system with potentials $(v(\mathbf{r}), V, \Psi)$. Following

the standard KS procedure, the xc potentials of the iq-DFT framework are then defined as

$$v_{\text{Hxc}}[n, I, Q](\mathbf{r}) = v_s[n, I, Q](\mathbf{r}) - v[n, I, Q](\mathbf{r}), \quad (11a)$$
$$V_{\text{xc}}[n, I, Q] = V_s[n, I, Q] - V[n, I, Q], \quad (11b)$$
$$\Psi_{\text{xc}}[n, I, Q] = \Psi_s[n, I, Q] - \Psi[n, I, Q]. \quad (11c)$$

The self-consistent coupled KS equations for the densities read ($\int \equiv \int_{-\infty}^{\infty}\frac{d\omega}{2\pi}$ in the following)

$$n(\mathbf{r}) = 2\sum_{\alpha=L,R}\int f\left(\frac{\omega - \mu_{s,\alpha}}{T_{s,\alpha}}\right)A_{s,\alpha}(\mathbf{r}, \omega), \quad (12a)$$

$$I = 2\sum_{\alpha=L,R}\int f\left(\frac{\omega - \mu_{s,\alpha}}{T_{s,\alpha}}\right)s_\alpha\mathcal{T}_s(\omega), \quad (12b)$$

$$Q = 2\sum_{\alpha=L,R}\int f\left(\frac{\omega - \mu_{s,\alpha}}{T_{s,\alpha}}\right)s_\alpha(\omega - \mu_{s,L})\mathcal{T}_s(\omega), \quad (12c)$$

where $f(x) = [1 + \exp(x)]^{-1}$ is the Fermi function, $\mu_{s,\alpha} = \mu + V_{s,\alpha}$, $T_{s,\alpha} = T(1 + s_\alpha\Psi_s/2)$, and $s_{L/R} = \pm 1$. We also defined the partial spectral function $A_{s,\alpha}(\mathbf{r}, \omega) = \langle\mathbf{r}|\mathcal{G}(\omega)\Gamma_\alpha(\omega)\mathcal{G}^\dagger(\omega)|\mathbf{r}\rangle$, with $\mathcal{G}(\omega)$ and $\Gamma_\alpha(\omega)$ the KS Green's function and broadening matrices, respectively, and the KS transmission function $\mathcal{T}_s(\omega) = \text{Tr}\{\mathcal{G}(\omega)\Gamma_L(\omega)\mathcal{G}^\dagger(\omega)\Gamma_R(\omega)\}$. Finally, the energy current follows directly from Eqs. (8) and (12):

$$W = 2\sum_{\alpha=L,R}\int f\left(\frac{\omega - \mu_{s,\alpha}}{T_{s,\alpha}}\right)s_\alpha\omega\mathcal{T}_s(\omega). \quad (13)$$

Equations (12a) and (12b) have the same structure as the KS equations of the original i-DFT formulation, except that in the present formalism the thermal gradient along the central region is not a parameter anymore but a basic potential which depends on the densities of the system. Therefore, the only possible parametric temperature dependence in the approximations for the functionals Eqs. (11) is through the average temperature T.

III. LINEAR RESPONSE

In this section, we develop the linear response formalism for iq-DFT which leads to expressions for the linear transport coefficients G, S, and κ purely in terms of quantities accessible by the theory.

The linear relationship for small variations of the basic densities around zero currents follows Eq. (4). The same current variations can be expressed in terms of the KS system

$$\begin{pmatrix} I \\ Q \end{pmatrix} = \mathbf{L}_s\begin{pmatrix} V + V_{\text{xc}} \\ \Psi + \Psi_{\text{xc}} \end{pmatrix}, \quad (14)$$

where we have used the definition of the KS potentials Eqs. (11) and that $I_s = I$ and $Q_s = Q$ by the KS construction. In the linear response regime, the changes in the xc potentials can be written as

$$\begin{pmatrix} V_{\text{xc}} \\ \Psi_{\text{xc}} \end{pmatrix} = \mathbf{F}_{\text{xc}}\begin{pmatrix} I \\ Q \end{pmatrix}, \quad (15)$$

with the matrix of xc derivatives $\mathbf{F}_{xc}$ defined by

$$\mathbf{F}_{xc} = \begin{pmatrix} \frac{\partial V_{xc}}{\partial I} & \frac{\partial V_{xc}}{\partial Q} \\ \frac{\partial \Psi_{xc}}{\partial I} & \frac{\partial \Psi_{xc}}{\partial Q} \end{pmatrix}\Bigg|_{\substack{I=0 \\ Q=0}}. \tag{16}$$

Combining Eqs. (4), (14), and (16), and using the fact that V and Ψ are arbitrary, we arrive at the Dyson equation

$$\mathbf{L} = \mathbf{L}_s + \mathbf{L}_s \mathbf{F}_{xc} \mathbf{L} \tag{17}$$

or, equivalently,

$$\mathbf{F}_{xc} = \mathbf{L}_s^{-1} - \mathbf{L}^{-1} = \mathbf{R}_s - \mathbf{R}. \tag{18}$$

Here, $\mathbf{L}$ and $\mathbf{L}_s$ are the interacting and KS conductance matrices where each element is evaluated at $(V = 0, \Psi = 0)$ and $(V_s = 0, \Psi_s = 0)$, respectively. Similarly, $\mathbf{R} = \mathbf{L}^{-1}$ and $\mathbf{R}_s = \mathbf{L}_s^{-1}$ are the interacting and KS resistance matrices where each element is evaluated at $(I = 0, Q = 0)$. As a consequence of the Onsager's relations between the cross terms in the conductance matrices, from Eq. (18) it follows

$$\frac{\partial V_{xc}}{\partial Q}\Bigg|_{\substack{I=0 \\ Q=0}} = \frac{\partial \Psi_{xc}}{\partial I}\Bigg|_{\substack{I=0 \\ Q=0}}. \tag{19}$$

We can express the $\mathbf{F}_{xc}$ elements as function of the linear transport coefficients making use of Eqs. (5) and (18) for the interacting and the KS system:

$$\frac{\partial V_{xc}}{\partial I}\Bigg|_{\substack{I=0 \\ Q=0}} = \frac{1}{G_s} + T\frac{S_s^2}{\kappa_s} - \frac{1}{G} - T\frac{S^2}{\kappa}, \tag{20a}$$

$$\frac{\partial \Psi_{xc}}{\partial I}\Bigg|_{\substack{I=0 \\ Q=0}} = \frac{\partial V_{xc}}{\partial Q}\Bigg|_{\substack{I=0 \\ Q=0}} = \frac{S_s}{\kappa_s} - \frac{S}{\kappa}, \tag{20b}$$

$$\frac{\partial \Psi_{xc}}{\partial Q}\Bigg|_{\substack{I=0 \\ Q=0}} = \frac{1}{T\kappa_s} - \frac{1}{T\kappa}. \tag{20c}$$

These equations can be inverted to express the transport coefficients as

$$\kappa = \frac{\kappa_s}{1 - T\frac{\partial \Psi_{xc}}{\partial Q}\big|_{\substack{I=0 \\ Q=0}}\kappa_s}, \tag{21a}$$

$$S = \frac{S_s - \kappa_s \frac{\partial V_{xc}}{\partial Q}\big|_{\substack{I=0 \\ Q=0}}}{1 - T\frac{\partial \Psi_{xc}}{\partial Q}\big|_{\substack{I=0 \\ Q=0}}\kappa_s}, \tag{21b}$$

$$G = \frac{G_s}{1 - \left(\frac{\partial V_{xc}}{\partial I}\big|_{\substack{I=0 \\ Q=0}} + \frac{TS^2}{\kappa} - \frac{TS_s^2}{\kappa_s}\right)G_s}. \tag{21c}$$

Equations (21) are exact expressions for the interacting (linear) transport coefficients in any molecular transport setup. They express the many-body transport coefficients in terms of quantities which are fully accessible within iq-DFT, i.e., the xc derivatives evaluated at $(I = 0, Q = 0)$ and the KS transport coefficients. The transport coefficients in iq-DFT exhibit increasing complexity: while the thermal conductance κ [Eq. (21a)] only depends on the KS thermal conductance

κ_s and $\frac{\partial \Psi_{xc}}{\partial Q}$, the Seebeck coefficient depends on its KS contribution S_s, κ_s as well as the two xc derivatives, $\frac{\partial V_{xc}}{\partial Q}$ and $\frac{\partial \Psi_{xc}}{\partial Q}$. Finally, the electrical conductance depends on the three KS coefficients (κ_s, S_s, G_s) and the three xc derivatives through S and κ.

Using Eqs. (21) for the iq-DFT transport coefficients, we now briefly discuss the relation of iq-DFT to other DFT-based frameworks for the description of steady-state transport. First, we consider the simplest approximation which completely neglects the xc contributions to the transport coefficients, i.e., setting $V_{xc} \approx 0$ and $\Psi_{xc} \approx 0$. Then all linear transport coefficients reduce to the corresponding KS coefficients, i.e., we recover the standard LB-DFT approach. At the next level, we consider the relation to the original i-DFT formalism which is designed to give the exact electrical steady current. The i-DFT expression for the electrical conductance

$$G = \frac{G_s}{1 - \frac{\partial V_{xc}^{i-DFT}}{\partial I}\big|_{I=0} G_s} \tag{22}$$

is exact, just as the corresponding iq-DFT expression Eq. (21c). Thus, we can establish the exact relation

$$\frac{\partial V_{xc}^{i-DFT}}{\partial I}\Bigg|_{I=0} = \frac{\partial V_{xc}^{iq-DFT}}{\partial I}\Bigg|_{\substack{I=0 \\ Q=0}} + \frac{TS^2}{\kappa} - \frac{TS_s^2}{\kappa_s} \tag{23}$$

for the current derivatives at $I = 0$ of the xc bias in i-DFT and iq-DFT. In the original i-DFT framework, the Seebeck coefficient as well as the thermal conductance are given by their KS counterparts. In iq-DFT, this corresponds to the approximation of setting $\Psi_{xc} \approx 0$ and approximating the xc bias as a functional independent of the heat current, i.e., $V_{xc}[n, I, Q] \approx V_{xc}[n, I]$. In earlier work [29], we have extended the original i-DFT formalism to not only give the many-body electrical conductance but also the many-body Seebeck coefficient, while for the thermal conductance one still has $\kappa = \kappa_s$. In iq-DFT, this corresponds to the approximation $\Psi_{xc}[n, I, Q] \approx \Psi_{xc}[n, I]$, independent of Q for general $V_{xc}[n, I, Q]$. Then we find $S = S_s - \kappa_s \frac{\partial V_{xc}}{\partial Q}\big|_{\substack{I=0 \\ Q=0}} = S_s + \frac{\partial V_{xc}}{\partial \Delta T}\big|_{\substack{I=0 \\ Q=0}} = S_s + S_{xc}$, as in Refs. [29,34]. This approximation then also implies a finite correction (over pure i-DFT) for the electrical conductance $G = G_s[1 - (\frac{\partial V_{xc}}{\partial I}\big|_{\substack{I=0 \\ Q=0}} + TS_{xc}(S_{xc} - 2S_s)/\kappa_s)G_s]^{-1}$.

To calculate the interacting transport coefficients from Eq. (21), one first needs to evaluate the KS coefficients and, consequently, an approximation for the functional $v_{Hxc}[n]$ is required where the dependence of v_{Hxc} on I and Q can be neglected if we work in the linear response regime. To gain some initial insight into the possible approximations for the iq-DFT functionals, in the following section we will discuss an application of iq-DFT formalism to a particular model system in the linear response regime.

IV. APPLICATION TO THE SINGLE IMPURITY ANDERSON MODEL

In this section, we apply our iq-DFT framework to the SIAM. Due to its simplicity and evident physical interpretation, this model is ideally suited as a system to explore the formalism and has been used in many previous works

[28,34,35], both within and outside any DFT setting. The SIAM describes a single interacting impurity (quantum dot) coupled to noninteracting left (*L*) and right (*R*) leads. The Hamiltonian of the system reads

$$\hat{H} = \sum_\sigma v\hat{n}_\sigma + U\hat{n}_\uparrow \hat{n}_\downarrow + \sum_{\alpha k \sigma} \varepsilon_{\alpha k \sigma} \hat{c}_{\alpha k \sigma}^\dagger \hat{c}_{\alpha k \sigma}$$
$$+ \sum_{k\alpha} (t_{\alpha k} \hat{c}_{\alpha k \sigma}^\dagger \hat{d}_\sigma + \text{H.c.}). \tag{24}$$

The first two terms in Eq. (24) describe the single impurity, where v is the on-site energy of the dot and U is the Coulomb interaction. $\hat{c}_{\alpha k \sigma}^\dagger$ and $\hat{d}_\sigma^\dagger$ are the creation operators for electrons with spin σ ($\sigma = \uparrow, \downarrow$) in lead α and on the dot, respectively. $\hat{n}_\sigma = \hat{d}_\sigma^\dagger \hat{d}_\sigma$ and $\hat{n} = \hat{n}_\uparrow + \hat{n}_\downarrow$ are the operators for the spin density and for the total density of electrons on the dot. The third and last term account for the single particle eigenstates of the isolated leads as well as for the tunneling between the dot and the leads with couplings $\Gamma_\alpha(\omega) := 2\pi \sum_k |t_{\alpha k}|^2 \delta(\omega - \varepsilon_{k\alpha})$. We consider featureless electronic leads described by frequency-independent couplings $\Gamma_\alpha(\omega) = \gamma_\alpha$ (with $\alpha = L, R$), i.e., we work in the wide band limit. For simplicity, we choose symmetric coupling of the leads, i.e., $\gamma_L = \gamma_R = \gamma/2$. In the present section, we are mostly concerned with application of the theory to the linear response regime, but for derivation purposes we keep a finite symmetric thermal gradient and a finite symmetric DC bias between the leads, i.e., $T_\alpha = T(1 + s_\alpha \frac{\Psi}{2})$ and $V_\alpha = s_\alpha \frac{V}{2}$ with $s_{L/R} = \pm 1$, where we choose $\mu = 0$.

A. Reverse engineering from a many-body model

To apply our iq-DFT formalism to the SIAM, we need approximations for all the xc potentials of the formalism. Since here we are concerned with the linear response regime only, we actually need to construct parametrizations for the derivatives of the xc potentials (at zero currents) appearing in Eqs. (21).

This can be achieved through a reverse engineering process. First, we express the interacting density on and currents through the dot in terms of the many-body spectral function $A(\omega)$ [36,37]:

$$n = \sum_{\alpha=L,R} \int f\left(\frac{\omega - s_\alpha \frac{V}{2}}{T(1 + s_\alpha \frac{\Psi}{2})}\right) A(\omega), \tag{25a}$$

$$I = \frac{\gamma}{2} \sum_{\alpha=L,R} \int s_\alpha f\left(\frac{\omega - s_\alpha \frac{V}{2}}{T(1 + s_\alpha \frac{\Psi}{2})}\right) A(\omega), \tag{25b}$$

$$Q = \frac{\gamma}{2} \sum_{\alpha=L,R} \int s_\alpha f\left(\frac{\omega - s_\alpha \frac{V}{2}}{T(1 + s_\alpha \frac{\Psi}{2})}\right)\left(\omega - \frac{V}{2}\right) A(\omega). \tag{25c}$$

To proceed with the reverse engineering, we consider the following model for the many-body spectral function [38] which correctly describes the impurity coupled to the leads in the parameter range $T/\gamma > 1$:

$$A(\omega) = \left(1 - \frac{n}{2}\right)\frac{\gamma}{(\omega - v)^2 + \frac{\gamma^2}{4}} + \frac{n}{2}\frac{\gamma}{(\omega - v - U)^2 + \frac{\gamma^2}{4}}. \tag{26}$$

In the following, we denote the spectral function of Eq. (26) as a many-body model (MBM). This model can be derived from the equations of motion technique [39]. However, it may also be understood more intuitively by calculating the exact spectral function of the single site model (SSM) [40], i.e., the limit of the uncontacted impurity. Broadening the delta peaks of the SSM spectral function to Lorentzian peaks with width given by the coupling strength γ, one obtains Eq. (26). The validity of this model is formally limited to temperatures larger than any other energy scale of the system. In particular, Eq. (26) correctly captures Coulomb blockade physics, but not the Kondo regime.

For the reverse engineering, we also need the densities and currents expressed through the KS equations. These can be obtained from Eqs. (25) by replacing the basic potentials by their noninteracting versions, i.e., $v \to v_s$, $V \to V_s$, and $\Psi \to \Psi_s$, and replacing $A(\omega) \to A_s(\omega) = \gamma/((\omega - v_s)^2 + \gamma^2/4)$. The resulting integrals can be evaluated analytically (see Appendix) and the basic variables of the theory can then be expressed as

$$n = 1 - \frac{1}{\pi}\left(\text{Im}\left[\psi\left(z_s^R\right)\right] + \text{Im}\left[\psi\left(z_s^L\right)\right]\right), \tag{27a}$$

$$I = \frac{\gamma}{2\pi}\left(\text{Im}\left[\psi\left(z_s^R\right)\right] - \text{Im}\left[\psi\left(z_s^L\right)\right]\right), \tag{27b}$$

$$Q = \frac{\gamma^2}{2\pi}\left(\text{Re}\left[\psi\left(z_s^L\right)\right] - \text{Re}\left[\psi\left(z_s^R\right)\right]\right)$$
$$+ \frac{\gamma^2}{2\pi}\ln\left(\frac{1 + \Psi_s/2}{1 - \Psi_s/2}\right) + \left(v_s - \frac{V_s}{2}\right)I, \tag{27c}$$

where $z_s^{L/R} = \frac{1}{2} + \frac{\gamma/2 + i(v_s \mp V_s/2)}{2\pi T(1 \pm \Psi_s/2)}$ and $\psi(z) = \frac{d\ln(\Gamma(z))}{dz}$ is the digamma function with general complex argument z, and $\Gamma(z)$ is the gamma function [41]. Also for our model many-body spectral function Eq. (26), all integrals in Eqs. (25) can be evaluated analytically using the same integrals of the Appendix but here we refrain from showing the resulting expressions explicitly.

Taking the derivatives in Eqs. (27) with respect to the related KS potentials, we can derive in an exact way the matrix elements L_{ij}^s of the matrix $\mathbf{L}_s$ [see Eq. (14)] as

$$L_{ij}^s(v_s) = M_{ij}(v_s), \tag{28}$$

where we have used the M_{ij} coefficients derived in Eqs. (A17) and made explicit the dependence on the KS potential v_s.

Similarly, also for the many-body model [Eq. (26) inserted into Eqs. (25)], we can derive the corresponding matrix elements of the interacting response matrix $\mathbf{L}$ by taking the corresponding derivatives. These matrix elements then read

$$L_{ij}(v) = \left(1 - \frac{n}{2}\right)M_{ij}(v) + \frac{n}{2}M_{ij}(v + U). \tag{29}$$

Combining Eqs. (6) and Eqs. (20), we arrive at

$$\frac{\partial V_{\text{xc}}}{\partial I}\bigg|_{\substack{I=0 \\ Q=0}} = \frac{1}{L_{11}^s(v_s)} - \frac{1}{L_{11}(v)} + \frac{L_{12}^s(v_s)^2}{L_{11}^s(v_s)}\frac{1}{\det(\mathbf{L_s}(v_s))}$$
$$- \frac{L_{12}(v)^2}{L_{11}(v)}\frac{1}{\det(\mathbf{L}(v))}, \tag{30a}$$

$$\frac{\partial \Psi_{\text{xc}}}{\partial I}\bigg|_{\substack{I=0 \\ Q=0}} = \frac{\partial V_{\text{xc}}}{\partial Q}\bigg|_{\substack{I=0 \\ Q=0}} = \frac{L_{12}^s(v_s)}{\det(\mathbf{L_s}(v_s))} - \frac{L_{12}(v)}{\det(\mathbf{L}(v))},$$

$$(30b)$$

$$\frac{\partial \Psi_{\text{xc}}}{\partial Q}\bigg|_{\substack{I=0 \\ Q=0}} = \frac{L_{11}^s(v_s)}{\det(\mathbf{L_s}(v_s))} - \frac{L_{11}(v)}{\det(\mathbf{L}(v))}.$$

$$(30c)$$

Equations (30) together with Eqs. (29) provide the analytical parametrizations of the xc derivatives in terms of both v_s and v. Instead, the dependence of the xc derivatives on the density can be obtained by (i) replacing v in the argument of the many-body coefficients L_{ij} by $v(n)$, the inverse of the density-potential relationship of Eq. (25a) (at $V = 0$ and $\Psi = 0$) and, similarly, (ii) by using $v_s(n)$ as arguments in the KS coefficients L_{ij}^s which can be obtained by inverting the corresponding KS expression $n(v_s)$ for the density (at $V_s = 0$ and $\Psi_s = 0$). These inverse functions can easily be obtained numerically and, by construction, the resulting density functionals for the xc derivatives then give exactly the same linear response transport coefficients (in a DFT framework) as the many-body model. Nevertheless, here we are interested in finding an analytical parametrization for the xc derivatives in terms of the density and therefore an approximation for the density-gate relationship is required.

Following ideas from previous works [40,42], we can refer to the SSM which describes a single (interacting or noninteracting) site not connected to leads but in contact with a heat and particle bath. The exact density-gate relations for the noninteracting and interacting SSM read

$$v_s(n) = T \ln\left(\frac{2}{n} - 1\right),$$

$$(31a)$$

$$v(n) = -U - T \ln\left(\frac{\delta n + \sqrt{\delta n^2 + e^{-\frac{U}{T}}(1 - \delta n^2)}}{1 - \delta n}\right),$$

$$(31b)$$

where $\delta n = n - 1$. The SSM may be viewed as the limiting case of a SIAM weakly coupled to leads and the Eqs. (31) become more accurate as the ratio T/γ increases [29]. Insertion of Eqs. (31) into Eqs. (30) defines our fully analytical parametrizations of the derivatives of the xc potentials of iq-DFT in the linear response regime. These functionals provide a measure of the correction required over the KS system to accurately describe the linear response properties of the many-body model. From Fig. 1, it is evident that the xc corrections become larger with increasing temperature T or interaction strength U. In the left column of Fig. 1, the xc derivatives are calculated at $U/\gamma = 8$ for different temperatures T while in the right column T is fixed to $T/\gamma = 12$ and the xc derivatives are obtained for different interactions U. Our analytical parametrization is compared with the numerically exact inversion from the MBM approach.

B. Numerical results

To assess the accuracy of our reverse-engineered approximations for the derivatives of the iq-DFT xc potentials in comparison to the reference MBM, we solve the DFT problem in the standard way. In the present paper, we use as an approximation for the Hxc (gate) potential the exact Hxc potential of
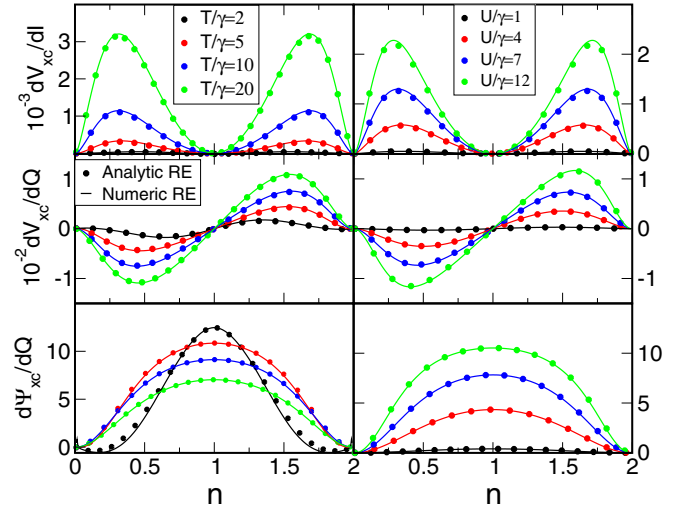

FIG. 1. Comparison between analytical and numerical reverse engineered xc derivatives as function of the density. The left column corresponds to $U/\gamma = 8$ and the right one to $T/\gamma = 12$. For the analytic result, the relation between the gates and the density from Eqs. (31) has been used, while for the numeric inversion this relation directly follows Eq. (27). The xc derivatives are obtained in both approaches using Eqs. (29) and (30).

the SSM [29,40] given as

$$v_{\text{Hxc}}^{\text{SSM}}(n) = v_s(n) - v(n),$$

$$(32)$$

with $v_s(n)$ and $v(n)$ of Eqs. (31a) and (31b), respectively. In Fig. 2, the iq-DFT densities as a function of the gate voltage ($v_g = v + \frac{U}{2}$) are compared with the ones obtained from MBM. As expected, this approximate Hxc potential works better as T/γ is increased (for fixed U/γ) while for relatively small $T/\gamma = 1$ the qualitative behavior of the density is captured well for different interactions while quantitative differences persist.

In Fig. 3, we show the linear transport coefficients for a fixed interaction strength $U/\gamma = 8$ and various temperatures
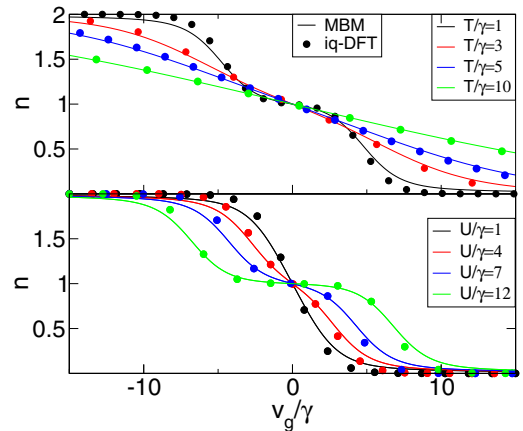

FIG. 2. Equilibrium density of the SIAM as a function of the gate voltage ($v_g = v + \frac{U}{2}$) from the MBM and iq-DFT. In iq-DFT, the Hxc potential of the single site model has been used (see main text). Upper panel: Density for different temperatures at fixed $U/\gamma = 8$. Lower panel: Density for different interactions at fixed $T/\gamma = 1$.
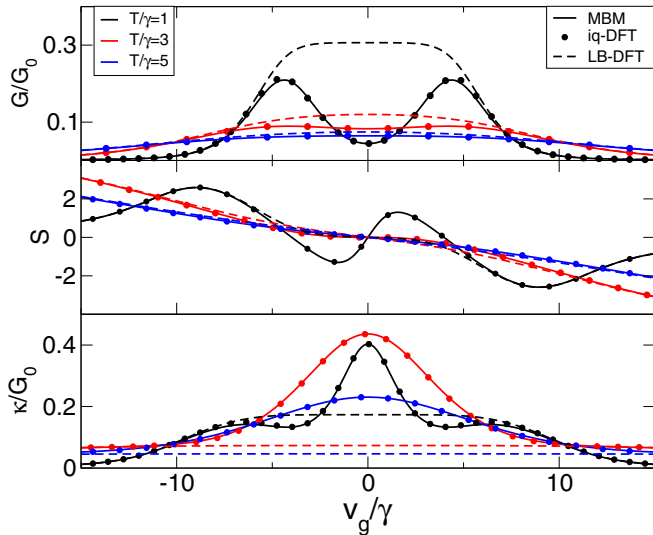
FIG. 3. Transport coefficients and electronic contribution to the figure of merit as a function of the gate voltage ($v_g = v + \frac{U}{2}$) for $U/\gamma = 8$. The iq-DFT results using the analytic reverse engineered xc derivatives Eqs. (30) are compared with those obtained directly from Eqs. (25) when using the model spectral function of Eq. (26).
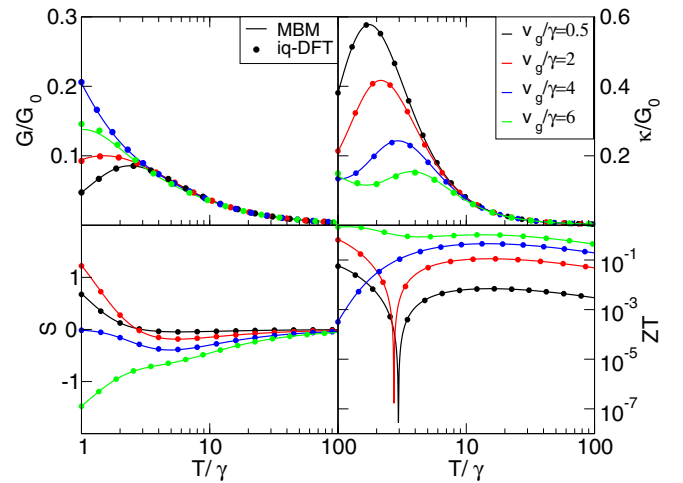

FIG. 4. Transport coefficients and electronic contribution to the figure of merit as a function of the temperature for $U/\gamma = 8$. The iq-DFT results using the analytic reverse engineered xc derivatives Eqs. (30) are compared with those obtained directly from Eqs. (25) when using the model spectral function of Eq. (26).

as function of the gate voltage v_g for the MBM, iq-DFT, and the LB-DFT approach (corresponding to the KS transport coefficients). The iq-DFT results agree extremely well with the MBM ones highlighting the good approximation of the gate-density relations [Eqs. (31)] in the range $T/\gamma > 1$. On the other hand, the LB-DFT results are only accurate in the empty orbital regime where correlations essentially play no role. Notice that, for $T/\gamma = 1$, in the LB-DFT the Seebeck coefficient flattens around $v_g/\gamma = 0$, while both iq-DFT and MBM predict a significant deviation [29,34]. Note that the electrical and heat conductances are shown in units of the quantum of conductance G_0, while the Seebeck coefficient is given in atomic units.

In Fig. 4, the iq-DFT transport coefficients as well as the figure of merit of the system $ZT = TGS^2/\kappa$ are compared with those obtained from MBM for fixed gate potential as a function of temperature for strong correlations $U/\gamma = 8$. As in Fig. 3, we observe excellent agreement as T/γ increases. Finally, in Fig. 5, we show the iq-DFT transport coefficients for different interaction strengths U using xc parametrizations [Eq. (30)]. Again we observe that for the given, fixed temperature $T/\gamma = 1$, the whole range from weak ($U/\gamma = 1$) to strong correlations ($U/\gamma > 7$) is correctly captured in iq-DFT as compared to the MBM.

In terms of summary of the numerical results, we have shown that our parametrization for the derivatives of the iq-DFT xc potentials leads to a rather accurate reproduction of the linear response transport coefficients of the MBM. There were two approximations involved in our iq-DFT approach: (i) we used the approximate Hxc potential of Eq. (32) for the self-consistent calculation of the density and (ii) the approximate density-potential relations Eq. (31) were used to construct the xc derivatives as functionals of the equilibrium density. Both approximations (i) and (ii) originate from the SSM and therefore it is not surprising that the corresponding iq-

DFT calculations show improved agreement with the MBM as temperature increases. We would also like to emphasize again that the MBM approximation for the spectral function Eq. (26) is by construction derived for the Coulomb blockade regime ($T/T_K \gg 1$ where T_K is the Kondo temperature of the system). Therefore, our approximation cannot and should not be expected to accurately describe the linear transport coefficients of the interacting system for temperatures in the Kondo regime ($T \ll T_K$). Nevertheless, our approximation may very well serve as a step toward the construction of improved approximations which are valid in this regime as well. While such a construction is beyond the scope of the present paper, we have already observed that the low-temperature behavior of the Seebeck coefficient and the thermal conductance are
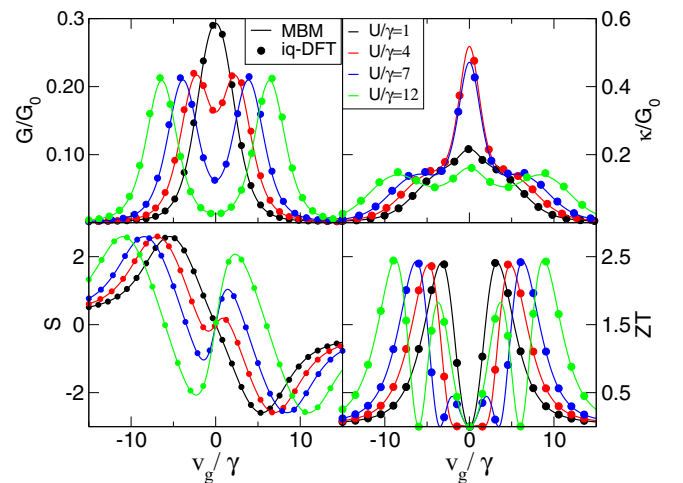

FIG. 5. Transport coefficients and electronic contribution to the figure of merit as function of the gate voltage ($v_g = v + \frac{U}{2}$) for $T/\gamma = 1$. The iq-DFT results using the analytic reverse engineered xc derivatives are compared with those obtained directly from Eqs. (25) when using the model spectral function of Eq. (26).

qualitatively correctly captured with the analytical approach. Therefore, the main corrections appear to be necessary for the electrical conductance, where ideas of the corresponding i-DFT construction [19] are expected to be transferable to iq-DFT as well. Before concluding, we would like to emphasize that the iq-DFT framework in principle is exact for both the Coulomb blockade and the Kondo regime and an improved approximation will cover both.

V. CONCLUSIONS

In this paper, we proposed a density functional framework, which we call iq-DFT, to describe both electronic and heat (energy) transport in the steady state for two-terminal (molecular) junctions driven out of equilibrium by an external bias and/or temperature gradient between the leads, generalizing our earlier i-DFT theory [18] for steady-state transport. The foundation of iq-DFT rests on the one-to-one correspondence between the set of three densities (n, I, Q) and the set of three potentials (v, V, Ψ), which we proved for a finite bias and thermal gradient window around equilibrium. Naturally, the corresponding KS system requires three xc potentials which need to be approximated in practice. Unlike i-DFT, iq-DFT allows us to calculate not only the density and steady current but also the heat current of interacting junctions. The widely used LB-DFT formalism may be viewed as a (crude) approximation to iq-DFT where the xc contributions to the bias as well as to the Ψ field are neglected completely and the xc contribution to the local (gate) potential is independent of the currents I and Q.

We developed the iq-DFT linear response formalism which allows us to access all linear thermal transport coefficients, i.e., the electrical conductance, the Seebeck coefficient, as well as the (electronic contribution to the) thermal conductance. All these coefficients can fully and exactly be expressed in terms of quantities accessible with iq-DFT, leading to xc corrections for all three transport coefficients. This goes beyond i-DFT, where only the electrical conductance [18] and the Seebeck cefficient [29] can exactly be written in terms of quantities of the theory.

As a first example, we applied iq-DFT in the linear response regime to the Anderson model. From reverse engineering of a MBM spectral function valid in the Coulomb blockade regime, we constructed fully analytical parametrizations of the derivatives of the iq-DFT xc potentials which accurately reproduce the transport coefficients of the many-body model. These parametrizations are expected to serve as a step toward construction of approximate xc functionals beyond the Coulomb blockade regime, in analogy to corresponding i-DFT work for the conductance [19].

As any DFT framework, due to the noninteracting nature of the KS system, iq-DFT can be expected to be a numerically highly efficient scheme for the *ab initio* calculation of current and heat transport through nanoscale systems as accurate approximations for the xc functionals become available.

APPENDIX: ANALYTIC EXPRESSIONS FOR THE TRANSPORT INTEGRALS IN THE SIAM

In this Appendix, we analytically evaluate the most important integrals needed both in the MBM and in the construction of our parametrization for the derivatives of the iq-DFT xc potentials. In our MBM for the SIAM, the many-body spectral function consists of two Lorentzians with broadening γ ($\gamma > 0$) centered at v and $v + U$, see Eqs. (26). Therefore, all integrals needed to compute the MBM density and currents have the form $\int d\omega \omega^n f(\omega) A(\omega)$ with $n = 0, 1$. The first integral we are interested in is

$$\mathcal{I}_1 = \int_{-\infty}^{\infty} f(x - V/2) \frac{\gamma}{(x - x_0)^2 + \frac{\gamma^2}{4}} dx, \quad \text{(A1)}$$

where the Fermi function $f(z)$ can be expanded as [43]

$$f(z) = \frac{1}{1 + e^{\frac{z}{T}}} = \frac{1}{2} - \frac{i}{2\pi} \sum_{n=0}^{\infty} \frac{1}{n + \frac{1}{2} + i\frac{z}{2\pi T}}. \quad \text{(A2)}$$

Using the substitution $x = V/2 + Tz$ and the abbreviations $a = \frac{x_0 - V/2}{T}$ and $b = \frac{\gamma}{2T}$, we can write the integral as

$$\mathcal{I}_1 = 2b \int_{-\infty}^{\infty} \frac{dz}{(e^z + 1)[(z - a)^2 + b^2]} \equiv 2b \int_{-\infty}^{\infty} g(z) dz. \quad \text{(A3)}$$

The integrand $g(z)$ has only single poles with nonvanishing imaginary part in the complex plane. We therefore use the calculus of residues to compute this integral. Since $g(z)$ vanishes sufficiently fast as $|z| \to \infty$, we can close the integration contour by a semicircle with infinite radius in the upper half plane (avoiding the poles on the imaginary axis). The integral then can be evaluated as

$$\mathcal{I}_1 = 4b\pi i \left[\frac{1}{i2b(e^{a+ib} + 1)} - \sum_{n=0}^{\infty} \frac{1}{[(2n+1)\pi i - a]^2 + b^2} \right]. \quad \text{(A4)}$$

For the terms in the sum, we perform a fractional decomposition and then use the series representation of the digamma function ψ,

$$\psi(z) = \sum_{n=0}^{\infty} \left(\frac{1}{n+1} - \frac{1}{n+z} \right) - \gamma^{\text{EM}}, \quad \text{(A5)}$$

with the Euler-Mascheroni constant $\gamma^{\text{EM}} \sim 0.5772$ to obtain

$$\mathcal{I}_1 = 2\pi \left[\frac{1}{e^{a+ib} + 1} - \frac{1}{2\pi i} \psi \left(\frac{1}{2} + \frac{b + ia}{2\pi} \right) \right.$$
$$\left. + \frac{1}{2\pi i} \psi \left(\frac{1}{2} + \frac{-b + ia}{2\pi} \right) \right]. \quad \text{(A6)}$$

We then apply the reflection formula

$$\psi(1 - z) = \psi(z) + \pi \cot(\pi z) \quad \text{(A7)}$$

to the last term and, returning to the original parameters, finally arrive at

$$\mathcal{I}_1(\gamma, x_0, V/2, T) = \pi - 2\,\mathrm{Im}\left[\psi\left(\frac{1}{2} + \frac{\frac{\gamma}{2} + \mathrm{i}(x_0 - V/2)}{2\pi T}\right)\right]. \tag{A8}$$

In the special case $x_0 = V/2$, $\mathcal{I}_1 = \pi$.

The second integral we are interested in is

$$\mathcal{I}_2 = \int_{-\infty}^{\infty} \mathrm{d}x \left(f\left(\frac{x - V/2}{1 + \Psi/2}\right) - f\left(\frac{x + V/2}{1 - \Psi/2}\right)\right)$$
$$\times \frac{x\gamma}{(x - x_0)^2 + \frac{\gamma^2}{4}}, \tag{A9}$$

where $\Psi = \frac{T_L - T_R}{T}$. We can rewrite $\mathcal{I}_2$ by decomposing the second factor as

$$\frac{x\gamma}{(x - x_0)^2 + \frac{\gamma^2}{4}} = \frac{\gamma}{2}[G^A(x) + G^R(x)]$$
$$- \mathrm{i}x_0[G^A(x) - G^R(x)], \tag{A10}$$

with the advanced and retarded Green's function $G^{A/R}(x) = \frac{1}{x - (x_0 \pm \mathrm{i}\frac{\gamma}{2})}$. Noting that the last term on the right-hand side of Eq. (A10) reduces to a Lorentzian, we obtain

$$\mathcal{I}_2 = \mathcal{I}_2^A + \mathcal{I}_2^R + x_0 \mathcal{I}_3, \tag{A11}$$

where $\mathcal{I}_3 = \mathcal{I}_1(\gamma, x_0, V/2, T_L) - \mathcal{I}_1(\gamma, x_0, -V/2, T_R)$ and we have defined

$$\mathcal{I}_2^{A/R} = \frac{\gamma}{2} \lim_{r \to \infty} \int_{-r}^{\infty} \mathrm{d}x\, G^{A/R}(x)$$
$$\times \left[f\left(\frac{x - V/2}{1 + \Psi/2}\right) - f\left(\frac{x + V/2}{1 - \Psi/2}\right)\right]. \tag{A12}$$

The integrals $\mathcal{I}_2^{A/R}$ are convergent because the difference of the Fermi functions decays asymptotically at least as x^{-1} as $|x| \to \infty$ and the Green's function contributes another asymptotic x^{-1} behavior in the same limit. Note that a lower cutoff has been explicitly introduced in Eq. (A12) to correctly account for the nonequivalent asymptotics of the two Fermi functions due to their generally different temperatures (in general, $\Psi \neq 0$).

By simple variable substitution, the integrals $\mathcal{I}_2^{A/R}$ can be written as

$$\mathcal{I}_2^{A/R} = \frac{\gamma}{2} \lim_{r \to \infty} \int_{\frac{-r + V/2}{1 - \Psi/2}}^{\infty} \mathrm{d}z\, f_T(z)$$

$$\times \left(\frac{1}{z + \frac{V/2 - (x_0 \pm \mathrm{i}\gamma/2)}{1 + \Psi/2}} - \frac{1}{z + \frac{-V/2 - (x_0 \pm \mathrm{i}\gamma/2)}{1 - \Psi/2}}\right)$$
$$+ \frac{\gamma}{2} \lim_{r \to \infty} \int_{\frac{-r - V/2}{1 + \Psi/2}}^{\frac{-r + V/2}{1 - \Psi/2}} \mathrm{d}z\, \frac{f_T(z)}{z + \frac{V/2 - (x_0 \pm \mathrm{i}\gamma/2)}{1 + \Psi/2}}. \tag{A13}$$

The first contribution can now again be evaluated by closing the contour with a semicircle in the upper half plane and summing the residues of all poles inside the contour which again leads to digamma functions. On the other hand, the second integral becomes trivial by replacing $f(z)$ with unity which is justified in the limit $r \to \infty$. This leads to

$$\mathcal{I}^A = \frac{\gamma}{2}\left[\psi\left(\frac{1}{2} + \frac{\gamma/2 - \mathrm{i}(x_0 - V/2)}{2\pi T_L}\right)\right.$$
$$\left. - \psi\left(\frac{1}{2} + \frac{\gamma/2 - \mathrm{i}(x_0 + V/2)}{2\pi T_R}\right)\right]$$
$$+ \frac{\gamma}{2} \ln\left(\frac{1 + \Psi/2}{1 - \Psi/2}\right) \tag{A14}$$

and

$$\mathcal{I}^R = \frac{\gamma}{2}\left[\psi\left(\frac{1}{2} + \frac{\gamma/2 + \mathrm{i}(x_0 - V/2)}{2\pi T_L}\right)\right.$$
$$\left. - \psi\left(\frac{1}{2} + \frac{\gamma/2 + \mathrm{i}(x_0 + V/2)}{2\pi T_R}\right)\right]$$
$$+ \frac{\gamma}{2} \ln\left(\frac{1 + \Psi/2}{1 - \Psi/2}\right). \tag{A15}$$

Using $\mathrm{Re}[\psi(a + \mathrm{i}b)] = \frac{1}{2}[\psi(a + \mathrm{i}b) + \psi(a - \mathrm{i}b)]$, we arrive at the final result for our second integral

$$\mathcal{I}_2 = \gamma\,\mathrm{Re}\left[\psi\left(\frac{1}{2} + \frac{\gamma/2 + \mathrm{i}(x_0 - V/2)}{2\pi T_L}\right)\right]$$
$$- \gamma\,\mathrm{Re}\left[\psi\left(\frac{1}{2} + \frac{\gamma/2 + \mathrm{i}(x_0 + V/2)}{2\pi T_R}\right)\right]$$
$$+ x_0 \mathcal{I}_3 + \gamma \ln\left(\frac{1 + \Psi/2}{1 - \Psi/2}\right). \tag{A16}$$

The results for the integrals of Eqs. (A8) and (A16) are sufficient to analytically evaluate the density and currents for the SIAM both in the MBM as well as in the KS system. With these integrals, we can also derive the analytical expressions for the integrals entering the transport coefficients in the linear response regime. These coefficients are

$$M_{11}(v) = \frac{\gamma}{4\pi} \frac{\mathrm{d}\mathcal{I}_3}{\mathrm{d}V}\bigg|_{\substack{V = 0 \\ \Psi = 0}} = \frac{-\gamma^2}{4\pi} \int f'(\omega) \frac{\mathrm{d}\omega}{(\omega - v)^2 + \frac{\gamma^2}{4}} = \frac{\gamma}{4\pi^2 T}\,\mathrm{Im}\left(\mathrm{i}\psi^{(1)}(z_1)\right), \tag{A17a}$$

$$M_{12}(v) = \frac{\gamma}{4\pi} \frac{\mathrm{d}\mathcal{I}_2}{\mathrm{d}V}\bigg|_{\substack{V = 0 \\ \Psi = 0}} = \frac{-\gamma^2}{4\pi} \int f'(\omega) \frac{\omega\,\mathrm{d}\omega}{(\omega - v)^2 + \frac{\gamma^2}{4}} = \frac{\gamma}{4\pi^2 T}\,\mathrm{Im}\left(z_0\psi^{(1)}(z_1)\right), \tag{A17b}$$

$$M_{22}(v) = \frac{\gamma}{4\pi} \frac{d\mathcal{I}_2}{d\Psi}\bigg|_{\substack{V = 0 \\ \Psi = 0}} = \frac{-\gamma^2}{4\pi} \int f'(\omega) \frac{\omega^2\,\mathrm{d}\omega}{(\omega - v)^2 + \frac{\gamma^2}{4}} = -\frac{\gamma^2}{8\pi^2 T}\,\mathrm{Re}\left(z_0\psi^{(1)}(z_1)\right) + vM_{12} + \frac{\gamma^2}{4\pi}, \tag{A17c}$$

where $z_0 = \frac{\gamma}{2} + \mathrm{i}v$, $z_1 = \frac{1}{2} + \frac{z_0}{2\pi T}$, and $\psi^{(1)}(z)$ is the trigamma function [41].

[1] H. J. Goldsmid, *Introduction to Thermoelectricity* (Springer, Berlin, 2010).

[2] G. Cuniberti, G. Fagas, and K. Richter, *Introducing Molecular Electronics* (Springer, Heidelberg, 2005).

[3] J. C. Cuevas and E. Scheer, *Molecular Electronics: An Introduction to Theory and Experiment* (World Scientific, London, 2010).

[4] M. Thoss and F. Evers, J. Chem. Phys. **148**, 030901 (2018).

[5] F. Evers, R. Korytár, S. Tewari, and J. M. van Ruitenbeek, Rev. Mod. Phys. **92**, 035001 (2020).

[6] B. Dutta, D. Majidi, N. W. Talarico, N. Lo Gullo, H. Courtois, and C. B. Winkelmann, Phys. Rev. Lett. **125**, 237701 (2020).

[7] E. Runge and E.K.U. Gross, Phys. Rev. Lett. **52**, 997 (1984).

[8] G. Stefanucci and C.-O. Almbladh, Phys. Rev. B **69**, 195318 (2004).

[9] G. Stefanucci and C.-O. Almbladh, Europhys. Lett. **67**, 14 (2004).

[10] N. Sai, M. Zwolak, G. Vignale, and M. Di Ventra, Phys. Rev. Lett. **94**, 186810 (2005).

[11] M. Koentopp, K. Burke, and F. Evers, Phys. Rev. B **73**, 121403(R) (2006).

[12] G. Stefanucci, S. Kurth, A. Rubio, and E. K. U. Gross, in *Molecular and Nano Electronics: Analysis, Design, and Simulation*, edited by J. Seminario (Elsevier, Amsterdam, 2006), Vol. 17.

[13] G. Vignale and M. Di Ventra, Phys. Rev. B **79**, 014201 (2009).

[14] F. G. Eich, M. Di Ventra, and G. Vignale, Phys. Rev. Lett. **112**, 196401 (2014).

[15] F. G. Eich, A. Principi, M. Di Ventra, and G. Vignale, Phys. Rev. B **90**, 115116 (2014).

[16] F. G. Eich, M. Di Ventra, and G. Vignale, J. Phys.: Condens. Matter **29**, 063001 (2017).

[17] F. Covito, F. G. Eich, R. Tuovinen, M. A. Sentef, and A. Rubio, J. Chem. Theory Comput. **14**, 2495 (2018).

[18] G. Stefanucci and S. Kurth, Nano Lett. **15**, 8020 (2015).

[19] S. Kurth and G. Stefanucci, Phys. Rev. B **94**, 241103(R) (2016).

[20] N. T. Maitra, K. Burke, and C. Woodward, Phys. Rev. Lett. **89**, 023002 (2002).

[21] N. T. Maitra, J. Chem. Phys. **144**, 220901 (2016).

[22] N. Dittmann, J. Splettstoesser, and N. Helbig, Phys. Rev. Lett. **120**, 157701 (2018).

[23] N. Dittmann, N. Helbig, and D. M. Kennes, Phys. Rev. B **99**, 075417 (2019).

[24] H. O. Wijewardane and C. A. Ullrich, Phys. Rev. Lett. **95**, 086401 (2005).

[25] R. D'Agosta and G. Vignale, Phys. Rev. Lett. **96**, 016405 (2006).

[26] D. Jacob and S. Kurth, Nano Lett. **18**, 2086 (2018).

[27] D. Jacob, G. Stefanucci, and S. Kurth, Phys. Rev. Lett. **125**, 216401 (2020).

[28] S. Kurth, D. Jacob, N. Sobrino, and G. Stefanucci, Phys. Rev. B **100**, 085114 (2019).

[29] N. Sobrino, R. D'Agosta, and S. Kurth, Phys. Rev. B **100**, 195142 (2019).

[30] L. Onsager, Phys. Rev. **37**, 405 (1931).

[31] H. B. Callen, Phys. Rev. **73**, 1349 (1948).

[32] D. Bohr, P. Schmitteckert, and P. Wölfle, Europhys. Lett. **73**, 246 (2006).

[33] M. A. Sierra and D. Sánchez, Mater. Today: Proc. **2**, 483 (2015).

[34] K. Yang, E. Perfetto, S. Kurth, G. Stefanucci, and R. D'Agosta, Phys. Rev. B **94**, 081410(R) (2016).

[35] M. I. Alomar, J. S. Lim, and D. Sánchez, Phys. Rev. B **94**, 165425 (2016).

[36] Y. Meir and N. S. Wingreen, Phys. Rev. Lett. **68**, 2512 (1992).

[37] T. A. Costi and V. Zlatić, Phys. Rev. B **81**, 235127 (2010).

[38] S. Kurth and G. Stefanucci, J. Phys.: Condens. Matter **29**, 413002 (2017).

[39] H. Haug and A.-P. Jauho, *Quantum Kinetics in Transport and Optics of Semiconductors* (Springer, New York, 2008).

[40] G. Stefanucci and S. Kurth, Phys. Rev. Lett. **107**, 216401 (2011).

[41] M. Abramowitz and I. A. Stegun, *Handbook of Mathematical Functions* (Dover, New York, 1965).

[42] N. Sobrino, S. Kurth, and D. Jacob, Phys. Rev. B **102**, 035159 (2020).

[43] A. L. Fetter and J. D. Walecka, *Quantum Theory of Many-Particle Systems* (Courier Corporation, New York, 2012).